Available online at BCREC website: https://bcrec.id

Bulletin of Chemical Reaction Engineering & Catalysis, 18 (4) 2023, 627-639

Research Article

Preparation, Characterization, and Photocatalytic Activity of Ni-Cd/Al_2O_3 Composite Catalyst

Yusmaniar Yusmaniar[1,*], Agung Premono[2], Ferry Budhi Susetyo[2], Sigit Dwi Yudanto[3]

[1]*Department of Chemistry, Faculty of Mathematics and Natural Sciences, Universitas Negeri Jakarta, Jln. Rawamangun Muka, Jakarta Timur 13220, Indonesia.*
[2]*Department of Mechanical Engineering, Faculty of Engineering, Universitas Negeri Jakarta, Jln. Rawamangun Muka, Jakarta Timur, 13220, Indonesia.*
[3]*Research Center for Metallurgy - National Research and Innovation Agency, KST B.J. Habibie, Serpong, 15314, Indonesia.*

Received: 29th September 2023; Revised: 28th October 2023; Accepted: 29th October 2023
Available online: 31st October 2023; Published regularly: December 2023

Abstract

This study was conducted to determine the effect of the radiation source and radiation time on the methylene blue (MB) solution by adding Ni-Cd/Al_2O_3 to the percent degradation of MB. To investigate similar purposes, the pH of the MB solution varied as well. The preparation, characterization, and photocatalytic activity of Ni-Cd/Al_2O_3 are three steps in this research. The Ni-Cd was prepared by mixing $Ni(NO_3)_2.6H_2O$ and $Cd(NO_3)_2.4H_2O$. Various concentrations of Ni-Cd were mixed with Al_2O_3, then heated, stirred, dried, and calcined to form Ni-Cd/Al_2O_3 powder. The dried powder catalysts were characterized using Field emission scanning electron microscopy (FESEM), Energy-dispersive X-ray spectroscopy (EDS), Brunauer-emmett-teller (BET), X-ray diffraction (XRD), Fourier transform infrared spectroscopy (FTIR), and Diffused reflectance spectrometer spectra (DR-UV-Vis). Higher degradation was observed at pH 11, when MB was degraded by 68% and 76% using the 5Ni-2Cd/Al_2O_3 and 6Ni-1Cd/Al_2O_3 catalysts, respectively. The 6Ni-1Cd/Al_2O_3 sample has higher absorption, less surface area, and less band gap; therefore, it has higher performance against degraded MB in the solution. In summary, 6Ni-1Cd/Al_2O_3 is capable of degrading MB and can be utilized in MB dye waste.

Keywords: Photodegradation; Methylene blue; Radiation source; Radiation time; pH

How to Cite: Y. Yusmaniar, A. Premono, F.B. Susetyo, S.D. Yudanto (2023). Preparation, Characterization, and Photocatalytic Activity of Ni-Cd/Al_2O_3 Composite Catalyst. *Bulletin of Chemical Reaction Engineering & Catalysis*, 18(4), 627-639 (doi: 10.9767/bcrec.20045)

Permalink/DOI: https://doi.org/10.9767/bcrec.20045

1. Introduction

Water pollution is an environmental issue related to hazardous wastes and toxics [1]. Several contaminants have a negative impact on the environment, and they are created by the emission of organic water pollutants, leading to a decrease in water quality. These pollutants are caused by various industries, such as primary metals, chemicals, food beverages, textiles, wood, pulp, and paper [2,3]. Organic dye, which is commonly produced from cloth and other industrial processes, is the main pollutant in wastewater [4,5]. There are several dye characteristics that are toxic, carcinogenic, teratogenic, harmful to human health, have high turbidity, and could decrease dissolved oxygen [6].

Methylene blue (MB) dyes, which are commonly used in the textile, printing, and pharmaceuticals industry, produce a high volume of wastewater in the environment and could be a

* Corresponding Author.
Email: yusmaniar@unj.ac.id (Y. Yusmaniar);
Telp: +62-21-4896669, Fax: +62-21-4894909

pollutant. The fact that water is essential for every living thing makes this condition a significant concern. Furthermore, the presence of MB in a water environment could result in eye damage to both humans and aquatic animals [7]. By eliminating and threatening MB dye pollution, there are numerous ways to solve this problem through sedimentation, oxidation, adsorption, filtration, and photocatalytic degradation [8–12]. Photocatalytic degradation is one of the most effective methods to degrade and remove pollutants because of its low cost and highly reactive technique [13–15]. Catalyst concentration, radiation source, time, and pH are all factors that have an impact on photocatalytic degradation [16,17].

Semiconductor materials, like CdS, NiO, TiO_2, ZnS and ZnO, have been utilized as photocatalysts [18]. The interfacial properties of the semiconductor bulk could be modified by semiconductor oxides prepared using the impregnation method of supporting oxides with a precursor compound [19]. The doping of the semiconductor metal is generally used to alter and improve the interfacial surface of the substrate material, improving the photocatalytic degradation reaction.

Numerous studies have been conducted on the synthesis of Ni/Cd materials. Kafeshani *et al.* [20] synthesized Ni-Cd co-doped $SrTiO_3$ photocatalysis through a co-precipitate method. Doped $SrTiO_3$ with 5wt% Ni-Cd could thoroughly degrade MB after 60 min of irradiation. Khan *et al.* [21] investigated the synergetic effect of $CdTiO_2$ and $NiCdTiO_2$ on the efficiency of photocatalytic TiO_2 nanoparticles. The photocatalytic activity demonstrated that TiO_2, $CdTiO_2$, and $NiCdTiO_2$ degraded MB by about 76.59, 82, and 86%, respectively. The presence of Cd and Ni could increase in the photocatalytic activity. This behavior was also found by Kebede *et al.* [22] that increasing coupled Ni-Cd concentration in $BiFeO_3$ enhanced the photocatalytic activity. Munawar *et al.* [23] prepared NiO-CdO-ZnO for photocatalytic activity in MB under solar light and found degradation of about 98% in 60 and 90 min illumination.

Al_2O_3 has also been conducted as a supported catalyst in various research due to its low cost [24]. Saffar *et al.* [25] synthesized novel $ZnAl_2O_4/Al_2O_3$ nanocomposite using sol-gel technique and found maximum MB removal around 70% under conditions: 10 mg/L MB, pH 8.5, 0.05 g of 70 wt% $ZnAl_2O_4/Al_2O_3$. Sodeifian and Behnood [26] synthesizing CuO/Al_2O_3 nanocomposite assist microwave irradiation in ethylene glycol. 90% of MB dye was successfully removed after 100 min using CuO/Al_2O_3 nanocomposite prepared with 900 W of microwave. Goudarzi *et al.* [27] synthesized $CuO/ZnO/Al_2O_3$ using $Cu(NO_3)_2$, $Zn(NO_3)_2$ and $Al(NO_3)_3$ with a molar ratio of 6:3:1. The photocatalytic activity shows about 70% of MB degraded after 50 min visible light irradiation. Sangor and Al-Ghouty [28] synthesized nano-g-Al_2O_3 from Al foil waste for efficient MB adsorption. Increasing the nano-g-Al_2O_3 concertation would increase the adsorption capacity of MB dye. Moreover, Al_2O_3 has an MB degradation efficiency of 65% and a rate constant of 8.4×10^{-3} s^{-1} [29].

Nallendran *et al.* [30] fabricated NiO-CdO and then added it to the methyl orange solution. Presenting NiO-CdO in the methyl orange solution would result in a photodegradation efficiency of around 89.44% when irradiated using visible light for 180 min. Balamurugan *et al.* [31] also synthesized and characterized CdO-Al_2O_3-NiO using the precipitation technique. The photodegradation efficiency of CdO-Al_2O_3-NiO in a metanil yellow solution is higher than Al_2O_3, CdO, and NiO. The research involved preparing, characterization, and investigating the photocatalytic activity of Ni-Cd/Al_2O_3 in MB, but it was not observed as stated above. Therefore, this study synthesizes different ratios of the coupled Ni and Cd metal, supported by Al_2O_3 base material. The Ni-Cd/Al_2O_3 samples were characterized with FESEM, EDS, BET, XRD, FTIR, and UV/Vis-DR spectroscopy. Various conditions, such as source light, radiation time, and pH, were also conducted for investigated MB degradation.

2. Materials and Methods

2.1 Materials

Commercial powder $(NO_3)_2.6H_2O$, $Cd(NO_3)_2.4H_2O$, and Al_2O_3 were purchased from Merck, while MB ($C_{16}H_{18}CIN_3S$) was acquired from Fluka Chemie AG CH-9470 Buchs as the starting materials for the study. Distilled water was utilized as a solvent in this experiment.

2.2 Synthesis of Photocatalyst Ni-Cd

The concentration of the Ni varied by 50 and 60 g/L (5 and 6 wt%). At the same time, Cd was varied by 10 and 20 g/L (1 and 2 wt%). 50 g/L of Ni l and 20 g/L of Cd were mixed and then designated 5Ni-2Cd. Moreover, 60 g/L of Ni and 10 g/L of Cd were mixed and then defined as 6Ni-1Cd. The mixed solution of 5Ni-2Cd and 6Ni-1Cd (50 mL) was renamed 5Ni-2Cd/Al_2O_3 and 6Ni-1Cd/Al_2O_3 after the addition of 25 g of Al_2O_3. Each mixture solution was heated at 85-90 °C and stirred continuously for 90 min. Subsequently, the catalyst was dried in the oven at 105 °C for 24 h. The photocatalyst was further calcined to activate and remove all the impurities. The activation process was carried out using a tube furnace at 600 °C with a continuous nitrogen flow rate of 20 cm³/min for 2 h. The various dried powder catalysts were used for further investigation. Figure 1 shows the schematic process synthesis of Ni-Cd/Al_2O_3.

2.3 Characterizations

The crystalline phases of Ni-Cd doped Al_2O_3 were examined using field emission scanning electron microscopy (FESEM) equipped with Energy Dispersive x-ray Spectroscopy (EDS) spectra by a Philips XL instrument using 25.0 kV. A Micromeritics Pulse ChemiSorb 2705 using 30% N_2: 70% O_2 was used to analyze Brunauer-Emmett-Teller (BET). The X-ray diffraction (XRD) analysis was carried out by a Siemens Diffractometer D5000 using Cu-Kα radiation at 30 mA and 40 kV. Fourier transform infrared spectroscopy (FTIR) analysis was carried out by a Perkin Elmer instrument using a KBr pelletizer with a scanning region of 400 - 4000 cm^{-1}. Moreover, a l90-diffused reflectance spectrometer was used to perform the UV-Vis spectra.

2.4 Photocatalytic Degradation of MB

2.4.1 Radiation source effect on MB photodegradation

The photodegradation of MB was carried out separately under UV light for 60 min, solar light at 10.00-11.00 AM, and in a dark room for 60 min. The 25 mL solution containing 20 mg/L MB + 50 mg of 5Ni-2Cd/Al_2O_3 was prepared to investigate the effect of the source of radiation photodegradation and then investigated with FTIR. Separately 20 mg/L MB + 50 mg of 6Ni-1Cd/Al_2O_3 was prepared and examined similarly. The percentage degradation of MB dyes was calculated using the following equation [32,33].

$$\%Degradation = \frac{(A_0 - A_t)}{A_0} \times 100\% \quad (1)$$

where, A_0 represents Initial absorption, and A_t represents absorption after t (min).

2.4.2 Radiation time effect on MB degradation rate

In order to investigate the effect of the radiation time on MB, a 50 mL solution was used with a concentration of 20 mg/L MB. The MB solution was added with 50 mg 5Ni-2Cd/Al_2O_3; another MB solution was added with 50 mg 6Ni-1Cd/Al_2O_3. Furthermore, the solutions were irradiated with UV light. Radiation was carried out for 180 min, and measurement of the degraded percentage of MB was performed

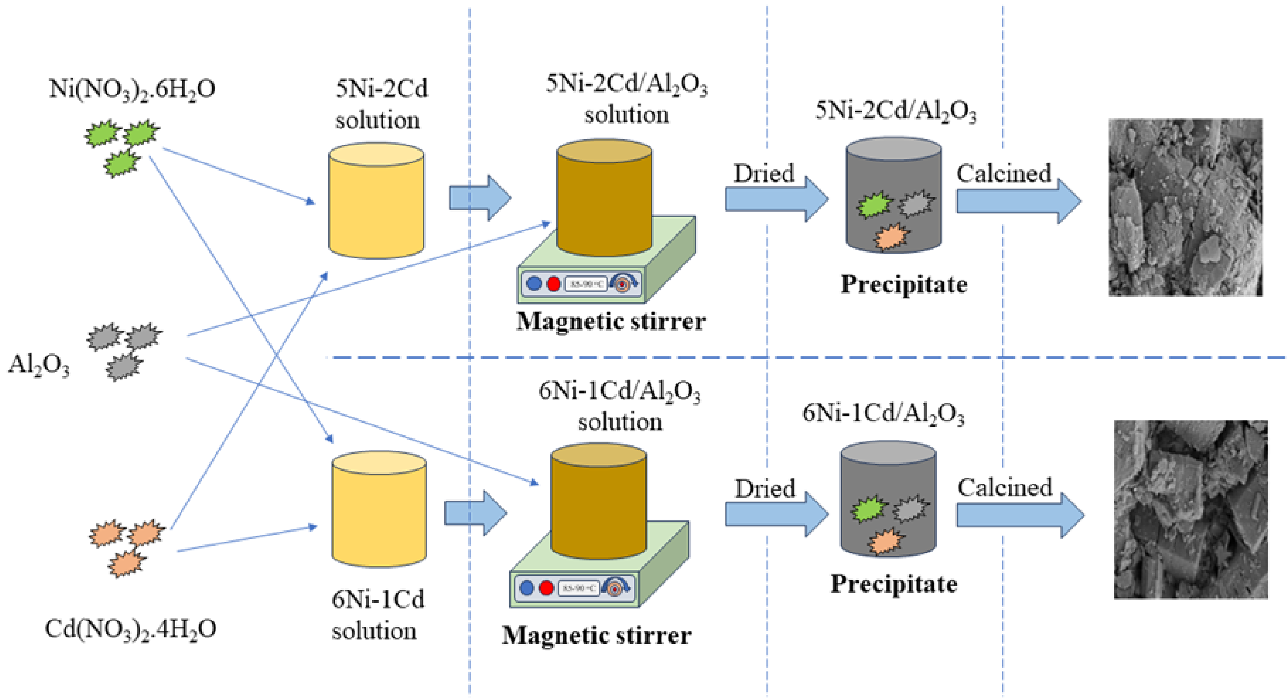

Figure 1. Schematic process Ni-Cd/Al_2O_3 synthesis.

at 0, 30, 60, 90, 120, 150, and 180 min using Equation (1).

2.4.3 pH Effect on the Degradation of MB

Various 20 mg/L MB of about 50 mL were prepared to determine the pH effect with a pH of 4, 6, 7, 9, 11, and 12. 50 mg of 5Ni-2Cd/Al_2O_3 and 6Ni-1Cd /Al_2O_3 were added to each MB solution. The mixed solution was added 0.1 M HCl until reached desired pH (4 and 6). Moreover 0.1 M NaOH was added into mixed solution to reach desired pH (7, 9, 11 and 12). Afterward each mixed solution was irradiated with UV light for 90 min.

3. Results and Discussion

3.1 Catalyst Characterizations

3.1.1 FESEM Analysis

The FESEM analysis was carried out on samples of Al_2O_3, 5Ni-2Cd/Al_2O_3, and 6Ni-1Cd/Al_2O_3. The Al_2O_3 result showed non-spherical and non-uniform particles with sharp edges (see Figure 2(a)). Moreover, adding Ni and Cd showed that particles filled the porous space of the Al_2O_3 (see Figure 2(b)). In contrast, the decrease in Cd concentration was not able to cover the porous area of Al_2O_3 (Figure 2(c)). Furthermore, a more compact morphology of CdO-Al_2O_3-NiO was seen in Balamurugan *et*

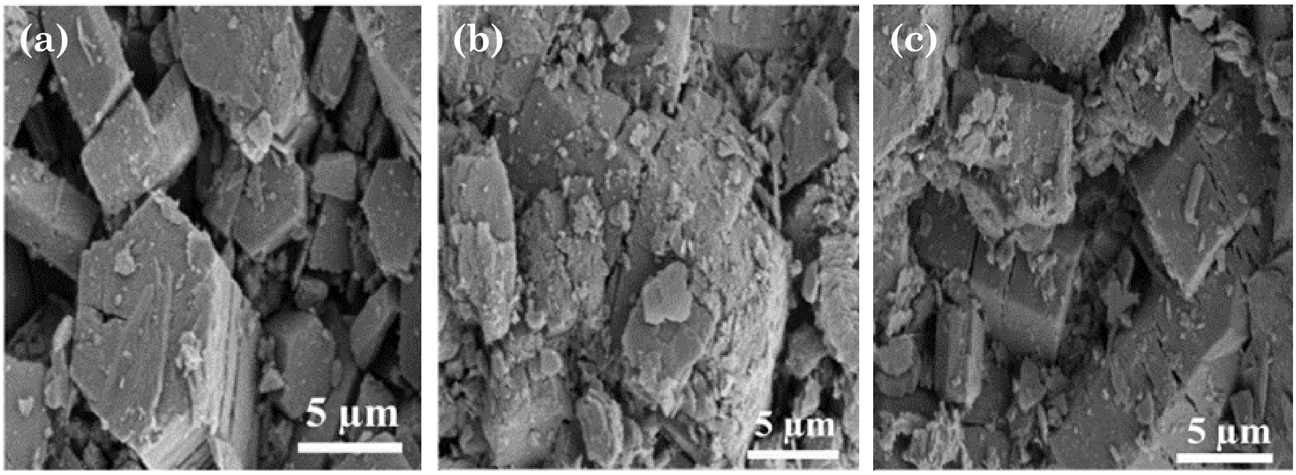

Figure 2. FESEM of (a) Al_2O_3, (b) 5Ni-2Cd/Al_2O_3 (c) 6Ni-1Cd/Al_2O_3.

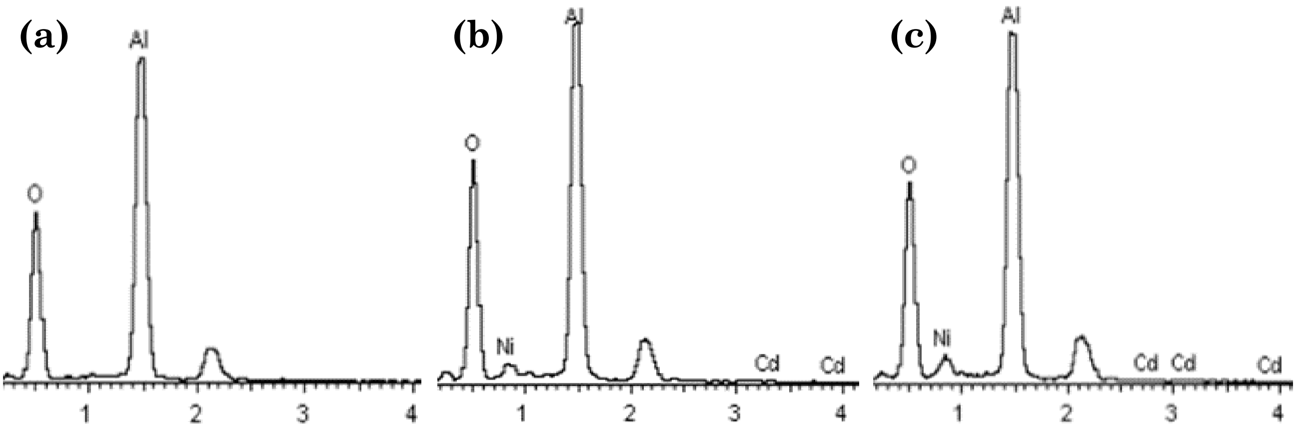

Figure 3. EDS spectrum of (a) Al_2O_3, (b)5Ni-2Cd/Al_2O_3 and (c) 6Ni-1Cd/Al_2O_3.

Table 1. EDS elemental analysis of samples.

Element	Composition (wt%)		
	Al_2O_3	5Ni-2Cd/Al_2O_3	6Ni-1Cd/Al_2O_3
O	47.50	46.21	45.21
Al	52.50	45.07	45.46
Ni	-	6.68	8.70
Cd	-	2.04	0.63
Total	100	100	100

al. [31] research due to the crushed process after calcination.

Isobe *et al.* [34] found agglomeration between Al_2O_3 and Ni with several voids fabricated by plasma sintering. Ni particles were observed between Al_2O_3 based on SEM investigation. Sahu *et al.* [35] investigated metal recovery from Ni-Cd cake waste residue by the hydrometallurgical route and found Zn, Ni, and Cd agglomerated based on an SEM study. Gürgenç *et al.* [36] fabricated thin films using NiO-CdO and found perfect agglomeration between them. Therefore, a mixture of Ni-Cd and Al_2O_3 could form a fusion between them.

3.1.2 EDS analysis

The EDS Spectroscopy was conducted to measure the percentage of element composition in the Al_2O_3, 5Ni-2Cd/Al_2O_3, and 6Ni1Cd/Al_2O_3. Figure 3 shows the EDS spectrum, while Table 1 shows the elements values in Al_2O_3, 5Ni-2Cd/Al_2O_3, and 6Ni-1Cd/Al_2O_3. The EDS result for Al_2O_3 reveals the presence of only Al and O elements. There are no impurities present in this sample. Four elements of the 5Ni-2Cd/Al_2O_3 and 6Ni-1Cd/Al_2O_3 catalysts were observed in the fabricated samples. When mixed with Ni-Cd, the percentage of Al and O decreased compared to pure alumina. Furthermore, the Ni and Cd in the 5Ni-2Cd/Al_2O_3 and 6Ni-1Cd/Al_2O_3 composites are confirmed to be perfectly placed in Al_2O_3. The EDS result suggests that Kebede *et al.* [22] behave similarly when co-doping Cd-Ni into $BiFeO_3$.

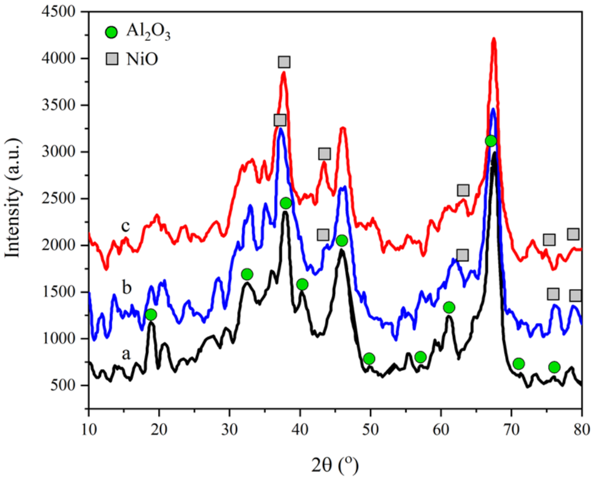

Figure 4. XRD diffractograms of (a) Al_2O_3, (b) 5Ni-2Cd/Al_2O_3 and (c) 6Ni-1Cd/Al_2O_3.

Table 2. BET surface area result.

No	Sample	Surface area (m^2/g)
1	5Ni-2Cd/Al_2O_3	88.32
2	6Ni-1Cd/Al_2O_3	77.32

3.1.3 BET surface area analysis

The BET results for Ni-Cd/Al_2O_3 are displayed in Table 2. The surface of 5Ni-2Cd/Al_2O_3 is found to be larger than that of 6Ni-1Cd/Al_2O_3. The surface area of the 6Ni-1Cd/Al_2O_3 photocatalyst decreased because the Cd particles did not fill the pores and cover the surface of Al_2O_3. This phenomenon was confirmed by the surface morphology of the FESEM investigation (Figure 2). Kafesyani *et al.* [20] found that the more porosity leads to a decrease in sample surface area. Moreover, Liu *et al.* [37] have similar findings; higher total pore volume leads to a reduced surface area.

3.1.4 XRD analysis

Figure 4(a)–(c) show the diffraction patterns for Ni-Cd doped alumina (Al_2O_3) samples. Based on the investigation, the Al_2O_3 phase can be identified in the diffraction pattern in Figure 4(a). In Figure 4(b) and (c), the diffraction pattern shows a peak at 2θ = 43.20°, indicating the semi-crystalline and cubic structure of the NiO phase. The peak of the NiO phase is comparable to those found in the study by Vishaka et al. [38]. Moreover, the entrapment of Ni-Cd in alumina led to the disappearance and degradation of several peaks (2θ = 27.1 and 60.8°). According to earlier research, the CdO phase peaks were found at 2θ of 38.24 and 55.23° [38]. The low Cd content of the samples was probably the cause of the absence of the CdO phase peaks in the Ni-Cd doped Al_2O_3.

3.1.5 FTIR analysis

FTIR was utilized to determine bond vibrations and demonstrate the presence of metal

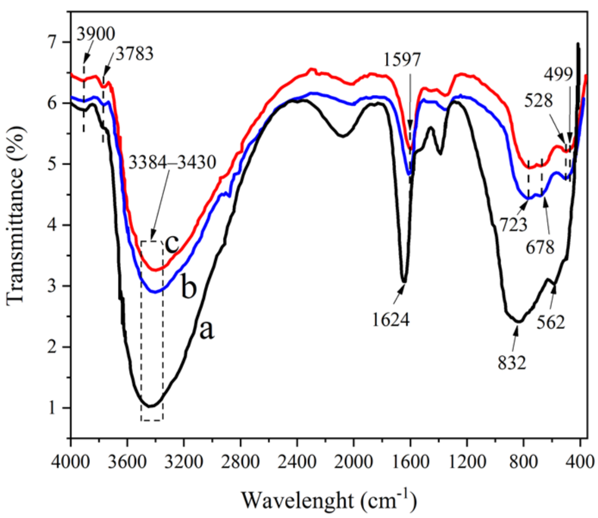

Figure 5. FTIR spectra of (a) Al_2O_3, (b) 5Ni-2Cd/Al_2O_3, and (c) 6Ni-1Cd/Al_2O_3.

oxide in the molecular structure. FTIR can identify the unknown materials and the functional groups present in the samples. The infrared spectra of fabricated Al_2O_3, 5Ni-2Cd/Al_2O_3, and 6Ni-1Cd/Al_2O_3 were recorded in 400-4000 cm^{-1} in the IR.

Figure 5 provides information on the FTIR spectra of Al_2O_3, 5Ni-2Cd/Al_2O_3, and 6Ni-1Cd/Al_2O_3. The obtained peak at 3900 cm^{-1} is related to the OH stretching mode [39]. The band received at 3783 cm^{-1} is associated with the stretching vibration of the hydroxyl groups of alumina [40]. The peak between 3384-3430 cm^{-1} represents the chemical bonding of the OH group [23]. The vibration band around 1624 cm^{-1} is because of the H_2O deformation vibration [41]. The band related to the symmetric bending vibration of the H_2O molecule is observed at 1597 cm^{-1} [42]. Two 832 and 562 cm^{-1} peaks correspond to the AlO stretching vibration bond [43]. The peak at 723 cm^{-1} is related to the CdO stretching vibration [44]. The band at 678 cm^{-1} is related to the NH bending mode [30]. The peak associated with the NiO bond is found at 528 cm^{-1} [30]. The peak attributed to the CdO stretching vibration can be seen at 499 cm^{-1} [41]. Thus, the NiO, CdO and AlO bonds in the Ni-Cd/Al_2O_3 composite catalyst confirmed their homogeneous mixing.

3.1.6 DR-UV-Vis analysis

The DR-UV-Vis is a technique that collects and analyzes scattered UV-Vis energy and measures the band gap energy of samples. In order to estimate the band gap energy, the absorption value of each specimen obtained was substituted to Planck's equation [45,46].

$$E_g = \frac{hc}{\lambda} = \frac{1240}{\lambda} \qquad (2)$$

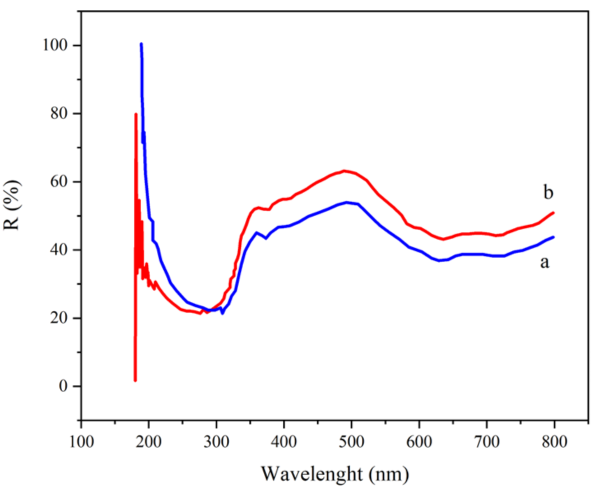

Figure 6. DR-UV-Vis spectra (a) 5Ni-2Cd/Al_2O_3 and (b) 6Ni-1Cd/Al_2O_3.

where, E_g is the band gap energy, h is the Planck constant, c is the velocity of light, and λ is the strong absorption edge.

The band gap energy value of 5Ni-2Cd/Al_2O_3 and 6Ni-1Cd/ Al_2O_3 was 4.42 and 3.875 eV, respectively. Farahmandjou and Montaghi [40] found that the pure alumina band gap has a value of 4.06 eV. Therefore, the band gap is narrowed by the addition of Ni-Cd. Boschloo and Hagfeldt [47] found that the NiO nanostructure (p-type semiconductor) has an indirect band gap of 3.55 eV. Przeździecka *et al.* [48] reported the CdO band gap value of 2.55 eV. Moreover, Nallendran *et al.* [30] found that pure NiO, CdO, and NiO-CdO equal 3.7, 2.47, and 3.1 eV, respectively. The NiO has a higher band gap than the CdO. Therefore, the catalyst with a higher Cd composition would result in a lower band gap, which is a perfect agreement with the present research.

Figure 6 shows the DR-UV-Vis spectra of 5Ni-2Cd/Al_2O_3 and 6Ni-1Cd/Al_2O_3, indicating the influence of Ni and Cd doping on the alumina support in the DR-UV-Vis absorption. Furthermore, the absorption spectrum of 6Ni-1Cd/Al_2O_3 showed a higher absorption at the UV-Vis region than to 5Ni-2Cd/Al_2O_3. This increase in the width of the absorption area indicates a redshift. The number of Ni ions increases as the Ni concentration increases, resulting in an increase in the redshift. In addition to showing a redshift, the two samples of Ni-Cd/Al_2O_3 photocatalysts showed absorbance at 280-320 nm wavelength. An increase in redshift implies an increase in photocatalytic activity. In addition, the maximum shift wavelength of the sample can also be related to the shorter distance between the valence and conduction bands. Thus, the process of forming hole pairs (h^+) and electrons is more optimal.

3.2 Photocatalytic Degradation of MB

3.2.1 Radiation source effect on photodegradation of MB

The effect of radiation sources on the MB degradation test aims is to determine the most effective radiation source to produce •OH radicals. Figure 7 shows that the percentage of MB degradation increases if the MB is stored in a dark space, irradiated by UV light and irradiated by solar light. Under dark conditions, MB has a lower degradation rate than UV or solar light radiation. In dark conditions, there is no radiation source; the energy of photons is very low, so too little •OH radicals are regenerated. MB is only absorbed on the surface of the catalyst, not degraded.

Alkaykh *et al.* [49] discovered that MB degradation in an aqueous solution with $MnTiO_3$ is higher when radiated with solar light than UV. This phenomenon is due to the optimal number of photons required for effective photocatalytic degradation attained under solar light [49]. Moreover, Zhang *et al.* [50] investigated the degradation of MB by adding pure PEDOT to MB solution under UV light and solar light radiation. They found that solar light radiation has more degradation of MB. The reason for this result is that PEDOT is capable of absorbing light and producing electrons, which leads to the separation and formation of oxyradicals [51]. As a result, the quantity of oxyradicals leads to a higher efficiency of MB degradation under solar light than UV light.

MB irradiated with solar light gives a higher degradation yield than UV light due to solar light having an intensity and wavelength between 310-2300 nm, greater than the wavelength of UV light around 200-380 nm [52–54]. In addition, solar light combines ±45% visible light and ±55% UV light. Therefore, solar light has relatively large energy and can provide photon energy to the photocatalyst [55]. When irradiated to energy above the band gap energy, a photocatalyst will produce holes that are potent oxidizing agents and make •OH radicals. These radicals break down MB into less complex compounds. Kafesyani [20] has preferred a sample with a lower band gap due to its high amounts of electrons, which leads to enhanced photocatalytic activity of the sample. As mentioned, the band gap energy value for $5Ni\text{-}2Cd/Al_2O_3$ and $6Ni\text{-}1Cd/Al_2O_3$ was 4.42 and 3.875 eV, respectively. Moreover, based on the absorption spectrum of $6Ni\text{-}1Cd/Al_2O_3$ showed higher absorption in the UV-Vis region compared to $5Ni\text{-}2Cd/Al_2O_3$. Therefore, the $6Ni\text{-}1Cd/Al_2O_3$ has a higher MB degradation in various source radiation.

Mebed *et al.* [56] investigated the degradation of MB by adding PbO-40% Al_2O_3 nanocomposites under visible and UV-visible light radiation. At 105 min of radiation time, the maximum degradation efficiency for visible and UV-visible light radiation sources are 26.5 and 25.5%, respectively. Compared to the present study, there was less degradation due to the larger band gap caused by Mebed *et al.* [56] research (4.61 eV). Moreover, Munawar *et al.* [23] investigated photocatalytic activity by adding NiO-CdO-ZnO in MB under solar light and found degradation of about 90% at 60 min of illumination. Compared to the current research, Munawar *et al.* [23] achieved higher degradation efficiency due to lower band gap (around 3.24 eV).

Another possible reason for $6Ni\text{-}1Cd/Al_2O_3$ having higher MB degradation in various source radiation is due to surface area. Based on BET measurements, $6Ni\text{-}1Cd/Al_2O_3$ has a smaller surface area than $5Ni\text{-}2Cd/Al_2O_3$. He *et al.* [10] found that decreased surface area of the catalyst leads to increased MB removal in the solution.

Figure 8 shows the FTIR spectra of MB with the fabricated $6Ni\text{-}1Cd/Al_2O_3$ in dark and UV light. The absorption peaks in the spectra have wavelengths that are almost the same. However, the transmittance values are significantly different. The result indicates the adsorption and degradation of MB by the fabricated $Ni\text{-}Cd/Al_2O_3$ photocatalyst. The FTIR spectrum of $MB+6Ni\text{-}1Cd/Al_2O_3$ in UV light shows higher IR absorption than that of $MB+6Ni\text{-}1Cd/Al_2O_3$ in dark conditions.

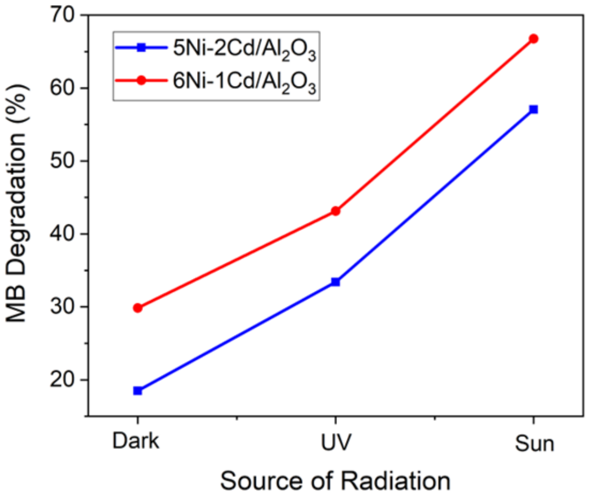

Figure 7. Effect of source radiation on MB degradation.

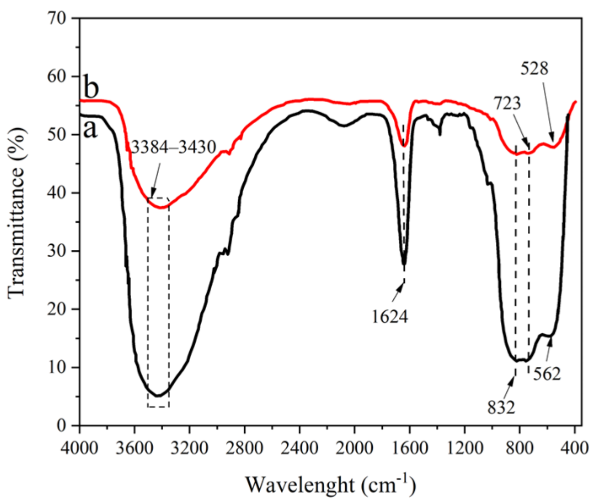

Figure 8. $MB+6Ni\text{-}1Cd/Al_2O_3$ FTIR spectra of (a) UV light and (b) Dark condition.

Based on Figure 8, the obtained peak between 3384-3430 cm^{-1} is the chemical bonding of the OH group [23]. The vibration band around 1624 cm^{-1} is caused by H_2O deformation vibration [41]. Two peaks of 832 and 562 cm^{-1} are associated with the vibration bond of AlO stretching [43]. The peak of 723 cm^{-1} is assigned as CdO stretching vibration [44]. The band at 528 cm^{-1} is associated with the NiO bond [30].

Compared to Figure 8 and 5, there are peaks that are missing at 3900, 3783, 1597, 678, and 499 cm^{-1}. This condition is probably due to the MB degradation process. Tzompantzi *et al*. [57] found similar behavior with the present research, where several peaks were missing due to degradation using 40 pp of phenol compared to 80 ppm of p-cresol. The comparison between Figures 5 and 8 show that the 6Ni-1Cd/Al_2O_3 catalyst remains stable after the MB degradation process due to almost similar spectra.

3.2.2 Radiation time effect on MB degradation rate

Figure 9 shows the effect of radiation time and catalyst type on MB percentage degradation. It can be seen that the longer the radiation time, the more MB is degraded. Alkaykh *et al*. [49] found that MB degradation in an aqueous solution by adding $MnTiO_3$ is increased by increasing the time. This condition is similar to that of solar light and UV radiation [49]. Balamurugan [31] investigated the MB degradation by adding CdO-Al_2O_3-NiO nanocomposite in the MB solution and found that MB degradation is increased by increasing the time. Similar behavior was also found in Zhang *et al*. [50] research when investigating the degradation of MB by adding pure PEDOT in the solution under solar light and UV light. Hence, it can be concluded that with increasing radiation time, more and more photon energy is absorbed by the catalyst on the surface, making it easier to degrade MB. Moreover, the degradation of the 5Ni-2Cd/Al_2O_3 sample is higher than that of 5Ni-2Cd/Al_2O_3; this requires further investigation.

The spectrum results for degradation MB with 5Ni-2Cd/Al_2O_3 and 6Ni-1Cd/Al_2O_3-based catalysts are shown in Figure 10. The UV-Vis investigation shows that the peak reduction for 5Ni-2Cd/Al_2O_3 is 43.21%, while 6Ni-1Cd/Al_2O_3 is about 24.53% at 675.08 nm in the decomposition of MB. According to Figures 10(a) and (b), no peaks shifted can be found, which suggests there was no generation of intermediates be-

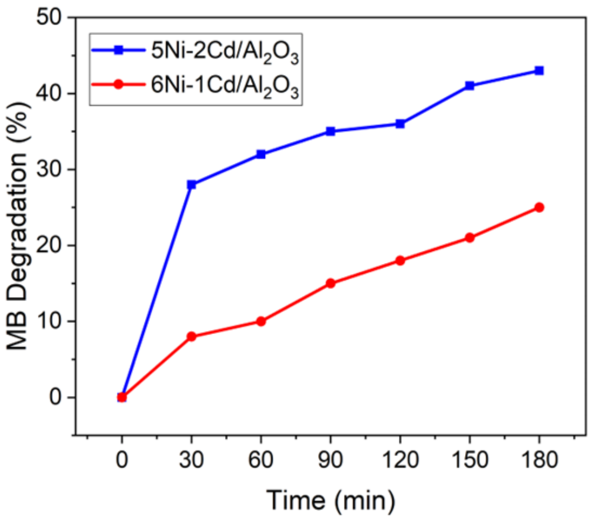

Figure 9. Radiation time effect on MB degradation by adding 5Ni2Cd/Al_2O_3 and 6Ni1Cd/Al_2O_3 separately.

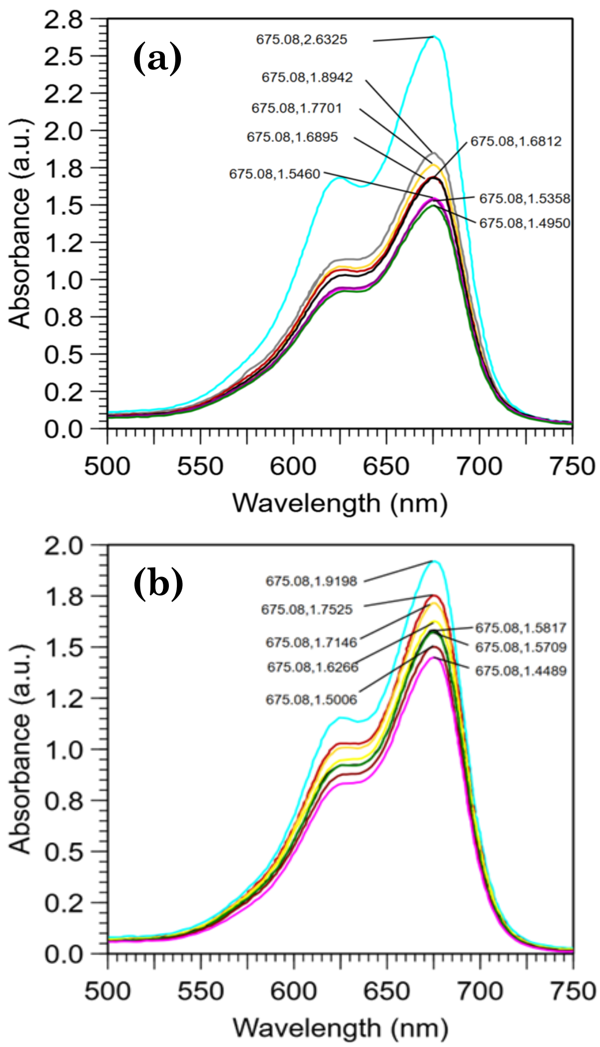

Figure 10. Spectrum of degradation of MB with (a) 5Ni-2Cd/Al_2O_3 and (b) 6Ni-1Cd/Al_2O_3 at UV illumination of 312 nm.

tween MB molecules and 5Ni-2Cd/Al_2O_3 or 6Ni-1Cd/Al_2O_3 catalyst during the interaction [10].

3.2.3 pH effect on the degradation of MB

In the degradation process, the pH value is essential. The pH value of a solution can affect the Ni-Cd surface charge ionic strength dye properties and the dye adsorption process on Ni-Cd/Al_2O_3 particles. In this study, the pH of the MB solution was maintained at 4, 6, 7, 9, 11, and 12 with a UV light irradiation time for 90 min. The results of pH optimization can be seen in Figure 11.

The decrease in the degradation rate at acidic pH may be due to the high adsorption at low pH. The catalyst surface is covered by dye molecules which causes the absorption of UV radiation on the surface of the catalyst to decrease [58]. In a low pH environment, it is also considered to be saturated with excess H^+ ions. Thereby inhibiting MB from being absorbed so that under acidic conditions, it can reduce the

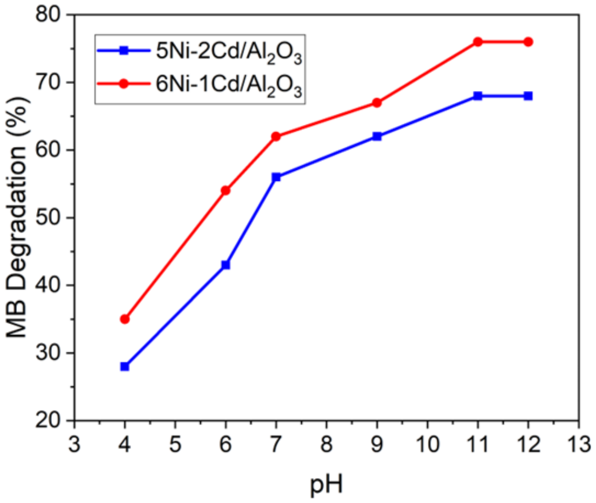

Figure 11. Effect of pH on degradation MB solution.

number of positive charges on the catalyst surface, facilitating the formation of hydroxyl radicals from the active catalyst [59]. An excess of ·OH anions at higher pH facilitates the photodegradation of •OH radicals. Changes in pH shift the redox potential of the valence and conduction bands which can affect interfacial charge transfer [58]. The effect of pH can be explained by the acid-base nature of the metal surface, which can be explained by the value of zero-point charge (ZPC). The adsorption of water molecules on the metal surface sites is followed by the dissociation of the charge of the OH^- group leading to the chemical equilibrium of the metal hydroxyl group (M−OH) according to the following reactions.

$$M{-}OH + H^+ \rightarrow M{-}OH^{2+} \quad (3)$$
$$M{-}OH \rightarrow M{-}O + H^+ \quad (4)$$

Equations (3) and (4) show the metal hydroxyl equilibrium reaction [60].

Several conditions, as mentioned in Table 3, have less degradation efficiency than present research. Moreover, Alkaykh *et al.* [49] found that MB degradation in an aqueous solution by $MnTiO_3$ is increased by increasing the pH. Tayyebi *et al.* [61] also found similar behavior when investigating bismuth vanadate's photoactivity. Therefore, photoactivity depends on pH, and MB degradation increases with increasing pH, which is identical to the present research.

4. Conclusions

Preparation, characterization, and photocatalytic activity of Ni-Cd/Al_2O_3 for MB degradation have been conducted. Due to more porosity, the 6Ni-1Cd/Al_2O_3 had a lesser surface area and higher absorption than the 5Ni-2Cd/Al_2O_3. A light source, time, and varied pH were proven to influence MB degradation. The

Table 3. Other research findings.

No	Research design	Result	Remark
1	0.002 g graphene oxide and b-cyclodextrin/graphene oxide to 50 mL MB solution (1.6 mg/L MB)	Degradation efficiency reached the maximum of 73 % (at pH value is 7)	Yang *et al.* [9]
2	Synthesized novel $ZnAl_2O_4/Al_2O_3$ nanocomposite and added it to MB solution	Maximum MB removal around 70% under conditions: 10 mg/L MB, pH 8.5, 0.05 g of 70 wt.% $ZnAl_2O_4/Al_2O_3$	Saffar *et al.* [25]
3	Synthesized nano-g-Al_2O_3 from aluminium foil waste, then 10 mg/L nano-g-Al_2O_3 added in MB solution with various pH values	Optimum degradation at pH 6 with 71% MB removal	Sangor and Al-Ghouti [28]

amount of oxyradicals results in higher efficiency of MB degradation under solar light than UV light. More and more photon energy are absorbed by the catalyst on the surface, making it easier to degrade MB by increasing radiation time. The highest MB degradation is found in pH 11 conditions by adding 6Ni-1Cd/Al_2O_3 catalyst in the solution because the 6Ni-1Cd/Al_2O_3 catalyst has a lower band gap than 5Ni-2Cd/Al_2O_3. Therefore, the 6Ni-1Cd/Al_2O_3 catalyst seems promising applied to the degradation of MB dye waste in industrial wastewater treatment.

Acknowledgments

This work was supported by BLU POK Faculty Mathematic and Natural Science Universitas Negeri Jakarta under contract No: 74 /SPK PENELITIAN/5.FMIPA//2020 The authors are grateful to my student Rini Pratiwi for technical assistance throughout this work.

CRediT Author Statement

Author Contributions: *Y. Yusmaniar*: Conceptualization of Research, Create Methodology, Investigation, Resources, Collected Data, Writing Draft Preparation, Review and Editing, Supervision, Validation; *A. Premono*: Conceptualization of Research, Methodology, Formal Analysis, Collected Data, Writing Draft Preparation, Project Administration; *F.B. Susetyo*: Validation, Writing, Review and Editing to template, Visualization; *S.D. Yudanto*: Investigation, Writing, Review and Editing to template, Visualization, Validation. All authors have read and agreed to the published version of the manuscript.

References

[1] Sagadevan, S., Fatimah, I., Egbosiub, T.C., Alshahateet, S.F., Lett, J.A., Weldegebrieal, G.K., Le, M.V., Johan, M.R. (2022). Photocatalytic Efficiency of Titanium Dioxide for Dyes and Heavy Metals Removal from Wastewater. *Bulletin of Chemical Reaction Engineering & Catalysis*, 17(2), 430–450. DOI: 10.9767/bcrec.17.2.13948.430-450.

[2] Hettige, H., Mani, M., Wheeler, D. (2000). Industrial Pollution in Economic Development: The Environmental Kuznets Curve Revisited. *Journal of Development Economics*, 62(2), 27–58. DOI: 10.1016/S0304-3878(00)00092-4.

[3] Hariharan, C. (2006). Photocatalytic degradation of organic contaminants in water by ZnO nanoparticles: Revisited. *Applied Catalysis A: General*, 304, 55–61. DOI: 10.1016/j.apcata.2006.02.020.

[4] Dharwal, M., Parashar, D., Shuaibu, M.S., Abdullahi, S.G., Abubakar, S., Bala, B.B. (2022). Water pollution: Effects on health and environment of Dala LGA, Nigeria. *Materials Today: Proceedings*, 49(8), 3036–3039. DOI: 10.1016/j.matpr.2020.10.496.

[5] Lestari, S., Muflihah, M., Kusumawardani, R., Nurhadi, M., Mangesa, Y., Ridho, F.I., Adawiyah, R., Ambarwati, P., Rahma, S., Yuan Lai, S., Nur, H. (2022). Activated Bledug Kuwu's Clay as Adsorbent Potential for Synthetic Dye Adsorption: Kinetic and Thermodynamic Studies. *Bulletin of Chemical Reaction Engineering & Catalysis*, 17(1), 22–31. DOI: 10.9767/bcrec.17.1.12473.22-31.

[6] Chung, K.-T. (2016). Azo Dyes and Human Health: A Review. *Journal of Environmental Science and Health, Part C*, 34(4), 233–261. DOI: 10.1080/10590501.2016.1236602.

[7] Sankar, M., Jothibas, M., Muthuvel, A., Rajeshwari, A., Jeyakumar, S.J. (2020). Structural, optical and Photocatalytic degradation of organic dyes by sol gel prepared Ni doped CdS nanoparticles. *Surfaces and Interfaces*, 21, 100775. DOI: 10.1016/j.surfin.2020.100775.

[8] Zhang, W., Huo, C., Hou, B., Lin, C., Yan, X., Feng, J., Yan, W. (2021). Secondary particle size determining sedimentation and adsorption kinetics of titanate-based materials for ammonia nitrogen and methylene blue removal. *Journal of Molecular Liquids*, 343, 117026. DOI: 10.1016/j.molliq.2021.117026.

[9] Yang, Z., Liu, X., Liu, X., Wu, J., Zhu, X., Bai, Z., Yu, Z. (2021). Preparation of β-cyclodextrin/graphene oxide and its adsorption properties for methylene blue. *Colloids and Surfaces B: Biointerfaces*, 200, 111605. DOI: 10.1016/j.colsurfb.2021.111605.

[10] He, Y., Jiang, D. Bin, Chen, J., Jiang, D.Y., Zhang, Y.X. (2018). Synthesis of MnO_2 nanosheets on montmorillonite for oxidative degradation and adsorption of methylene blue. *Journal of Colloid and Interface Science*, 510, 207–220. DOI: 10.1016/j.jcis.2017.09.066.

[11] Yu, F., Tian, F., Zou, H., Ye, Z., Peng, C., Huang, J., Zheng, Y., Zhang, Y., Yang, Y., Wei, X., Gao, B. (2021). ZnO/biochar nanocomposites via solvent free ball milling for enhanced adsorption and photocatalytic degradation of methylene blue. *Journal of Hazardous Materials*, 415, 125511. DOI: 10.1016/j.jhazmat.2021.125511.

[12] Huang, J., Peng, L., Zeng, G., Li, X., Zhao, Y., Liu, L., Li, F., Chai, Q. (2014). Evaluation of micellar enhanced ultrafiltration for removing methylene blue and cadmium ion simultaneously with mixed surfactants. *Separation and Purification Technology*, 125, 83–89. DOI: 10.1016/j.seppur.2014.01.020.

[13] Al-Hamdi, A.M., Rinner, U., Sillanpää, M. (2017). Tin dioxide as a photocatalyst for water treatment: A review. *Process Safety and Environmental Protection*, 107, 190–205. DOI: 10.1016/j.psep.2017.01.022.

[14] Bora Akin, M., Oner, M. (2013). Photodegradation of methylene blue with sphere-like ZnO particles prepared via aqueous solution. *Ceramics International*, 39(8), 9759–9762. DOI: 10.1016/j.ceramint.2013.05.024.

[15] Odling, G., Robertson, N. (2019). Bridging the gap between laboratory and application in photocatalytic water purification. *Catalysis Science and Technology*, 9(3), 533–545. DOI: 10.1039/c8cy02438c.

[16] Sun, S., Zhao, R., Xie, Y., Liu, Y. (2019). Photocatalytic degradation of aflatoxin B1 by activated carbon supported TiO_2 catalyst. *Food Control*, 100, 183–188. DOI: 10.1016/j.foodcont.2019.01.014.

[17] Wang, P., Yuan, Q. (2021). Photocatalytic degradation of tetracyclines in liquid digestate: Optimization, kinetics and correlation studies. *Chemical Engineering Journal*, 410, 128327. DOI: 10.1016/j.cej.2020.128327.

[18] Abdullah, N., Ayodele, B. V., Mansor, W.N.W., Abdullah, S. (2018). Effect of incorporating TiO_2 photocatalyst in PVDF hollow fibre membrane for photo-assisted degradation of methylene blue. *Bulletin of Chemical Reaction Engineering & Catalysis*, 13(3), 588–591. DOI: 10.9767/bcrec.13.3.2909.588-591.

[19] Zhang, H., Wang, X., Zhu, D., Zhao, J., Yang, T., Zhou, Y., Lu, J., Cai, C., Huang, J., Zhou, G. (2021). Interfacial oxidation of hafnium modified NiAl alloys. *Corrosion Science*, 189, 109604. DOI: 10.1016/j.corsci.2021.109604.

[20] Kafeshani, M.A., Mahdikhah, V., Sheibani, S. (2022). Facile preparation and modification of $SrTiO_3$ through Ni–Cd co-doping as an efficient visible-light-driven photocatalyst. *Optical Materials*, 133, 113080. DOI: 10.1016/j.optmat.2022.113080.

[21] Khan, S., Noor, A., Khan, I., Muhammad, M., Sadiq, M., Muhammad, N. (2023). Photocatalytic Degradation of Organic Dyes Contaminated Aqueous Solution Using Binary $CdTiO_2$ and Ternary $NiCdTiO_2$ Nanocomposites. *Catalysts*, 13(1), 44. DOI: 10.3390/catal13010044.

[22] Kebede, M.T., Devi, S., Dillu, V., Chauhan, S. (2022). Influence of novel Cd – Ni co-substitution on structural, magnetic, optical and photocatalytic properties of BiFeO3 nanoparticles. *Journal of Alloys and Compounds*, 894, 162552. DOI: 10.1016/j.jallcom.2021.162552.

[23] Munawar, T., Iqbal, F., Yasmeen, S., Mahmood, K., Hussain, A. (2020). Multi metal oxide NiO-CdO-ZnO nanocomposite–synthesis, structural, optical, electrical properties and enhanced sunlight driven photocatalytic activity. *Ceramics International*, 46(2), 2421–2437. DOI: 10.1016/j.ceramint.2019.09.236.

[24] Yadav, D., Kavaiya, A.R., Mohan, D., Prasad, R. (2017). Low temperature selective catalytic reduction (SCR) of NOx emissions by Mn-doped Cu/Al_2O_3 catalysts. *Bulletin of Chemical Reaction Engineering & Catalysis*, 12(3), 415–429. DOI: 10.9767/bcrec.12.3.895.415-429.

[25] Saffar, A., Ahangar, H.A., Salehi, S., Fekri, M.H., Rabbani, A. (2021). Synthesis of novel $ZnAl_2O_4/Al_2O_3$ nanocomposite by sol–gel method and its application as adsorbent. *Journal of Sol-Gel Science and Technology*, 99(1), 158–168. DOI: 10.1007/s10971-021-05559-1.

[26] Sodeifian, G., Behnood, R. (2017). Application of microwave irradiation in preparation and characterization of CuO/Al_2O_3 nanocomposite for removing MB dye from aqueous solution. *Journal of Photochemistry and Photobiology A: Chemistry*, 342, 25–34. DOI: 10.1016/j.jphotochem.2017.03.038.

[27] Goudarzi, M., Salavati-Niasari, M. (2018). Using pomegranate peel powders as a new capping agent for synthesis of $CuO/ZnO/Al_2O_3$ nanostructures; enhancement of visible light photocatalytic activity. *International Journal of Hydrogen Energy*, 43(31), 14406–14416. DOI: 10.1016/j.ijhydene.2018.06.034.

[28] Sangor, F.I.M.S., Al-Ghouti, M.A. (2023). Waste-to-value: Synthesis of nano-aluminum oxide (nano-γ-Al_2O_3) from waste aluminum foils for efficient adsorption of methylene blue dye. *Case Studies in Chemical and Environmental Engineering*, 8, 100394. DOI: 10.1016/j.cscee.2023.100394.

[29] Sridevi, A., Krishnamohan, S., Thairiyaraja, M., Prakash, B., Yokeshwaran, R. (2022). Visible-light driven γ-Al_2O_3, CuO and γ-Al_2O_3/CuO nanocatalysts: Synthesis and enhanced photocatalytic activity. *Inorganic Chemistry Communications*, 138, 109311. DOI: 10.1016/j.inoche.2022.109311.

[30] Nallendran, R., Selvan, G., Balu, A.R. (2018). Photoconductive and photocatalytic properties of CdO–NiO nanocomposite synthesized by a cost effective chemical method. *Journal of Materials Science: Materials in Electronics*, 29(13), 11384–11393. DOI: 10.1007/s10854-018-9227-5.

[31] Balamurugan, S., Balu, A.R., Narasimman, V., Selvan, G., Usharani, K., Srivind, J., Suganya, M., Manjula, N., Rajashree, C., Nagarethinam, V.S. (2019). Multi metal oxide CdO-Al_2O_3-NiO nanocomposite - Synthesis, photocatalytic and magnetic properties. *Materials Research Express*, 6(1), 015022. DOI: 10.1088/2053-1591/aae5af.

[32] Rahman, Q.I., Ahmad, M., Misra, S.K., Lohani, M. (2013). Effective photocatalytic degradation of rhodamine B dye by ZnO nanoparticles. *Materials Letters*, 91, 170–174. DOI: 10.1016/j.matlet.2012.09.044.

[33] Jawad, A.H., Alkarkhi, A.F.M., Mubarak, N.S.A. (2015). Photocatalytic decolorization of methylene blue by an immobilized TiO_2 film under visible light irradiation: optimization using response surface methodology (RSM). *Desalination and Water Treatment*, 56(1), 161–172. DOI: 10.1080/19443994.2014.934736.

[34] Isobe, T., Daimon, K., Sato, T., Matsubara, T., Hikichi, Y., Ota, T. (2008). Spark plasma sintering technique for reaction sintering of Al_2O_3/Ni nanocomposite and its mechanical properties. *Ceramics International*, 34(1), 213–217. DOI: 10.1016/j.ceramint.2006.08.017.

[35] Sahu, S.K., Razi, M.K., Beuscher, M., Chagnes, A. (2020). Recovery of metal values from ni-cd cake waste residue of an iranian zinc plant by hydrometallurgical route. *Metals*, 10(5), 655. DOI: 10.3390/met10050655.

[36] Gürgenç, E., Dıkıcı, A., Aslan, F. (2022). Investigation of structural, electrical and photoresponse properties of composite based Al/NiO:CdO/p-Si/Al photodiodes. *Physica B: Condensed Matter*, 639, 413981. DOI: 10.1016/j.physb.2022.413981.

[37] Liu, Y., Meng, Y., Qiu, X., Zhou, F., Wang, H., Zhou, S., Yan, C. (2023). Novel porous phosphoric acid-based geopolymer foams for adsorption of Pb(II), Cd(II) and Ni(II) mixtures: Behavior and mechanism. *Ceramics International*, 49(4), 7030–7039. DOI: 10.1016/j.ceramint.2022.10.164.

[38] Vishaka, E.J., Priya Dharshini, M., Shally, V., Gerardin Jayam, S. (2022). NiO-CdO nanocomposite for photocatalytic applications. *Materials Today: Proceedings*, 68, 294–298. DOI: 10.1016/j.matpr.2022.05.180.

[39] Caccamo, M.T., Mavilia, G., Mavilia, L., Lombardo, D., Magazù, S. (2020). Self-assembly processes in hydrated montmorillonite by FTIR investigations. *Materials*, 13(5), 1100. DOI: 10.3390/ma13051100.

[40] Farahmandjou, M., Motaghi, S. (2019). Sol–gel synthesis of Ce-doped α-Al_2O_3: Study of crystal and optoelectronic properties. *Optics Communications*, 441, 1–7. DOI: 10.1016/j.optcom.2019.02.029.

[41] Anitha, S., Suganya, M., Prabha, D., Srivind, J., Balamurugan, S., Balu, A.R. (2018). Synthesis and characterization of NiO-CdO composite materials towards photoconductive and antibacterial applications. *Materials Chemistry and Physics*, 211, 88–96. DOI: 10.1016/j.matchemphys.2018.01.048.

[42] Hakimi, M., Mardani, Z., Moeini, K. (2013). Spectral and geometrical study of two cadmium complexes, mer-R,S-[Cd(aepn)2]X2 (X: I-, Cl-, aepn: N-(2-Aminoethyl)-1,3-propanediamine) supported by solution experiments. *Journal of the Korean Chemical Society*, 57(4), 447–454. DOI: 10.5012/jkcs.2013.57.4.447.

[43] Jbara, A.S., Othaman, Z., Saeed, M.A. (2017). Structural, morphological and optical investigations of θ-Al_2O_3 ultrafine powder. *Journal of Alloys and Compounds*, 718, 1–6. DOI: 10.1016/j.jallcom.2017.05.085.

[44] Joyce Stella, R., Thirumala Rao, G., Pushpa Manjari, V., Babu, B., Rama Krishna, C., Ravikumar, R.V.S.S.N. (2015). Structural and optical properties of CdO/ZnS core/shell nanocomposites. *Journal of Alloys and Compounds*, 628, 39–45. DOI: 10.1016/j.jallcom.2014.11.201.

[45] Debanath, M.K., Karmakar, S. (2013). Study of blueshift of optical band gap in zinc oxide (ZnO) nanoparticles prepared by low-temperature wet chemical method. *Materials Letters*, 111, 116–119. DOI: 10.1016/j.matlet.2013.08.069.

[46] Vijeth, H., Ashokkumar, S.P., Yesappa, L., Vandana, M., Devendrappa, H. (2019). Photocatalytic degradation of methylene blue and Rhodamine B using polythiophene nanocomposites under visible and UV light. *AIP Conference Proceedings*, 2115, 030535. DOI: 10.1063/1.5113375.

[47] Boschloo, G., Hagfeldt, A. (2001). Spectroelectrochemistry of nanostructured NiO. *Journal of Physical Chemistry B*, 105(15), 3039–3044. DOI: 10.1021/jp003499s.

[48] Przeździecka, E., Strąk, P., Wierzbicka, A., Adhikari, A., Lysak, A., Sybilski, P., Sajkowski, J.M., Seweryn, A., Kozanecki, A. (2021). The Band-Gap Studies of Short-Period CdO/MgO Superlattices. *Nanoscale Research Letters*, 16(1), 59. DOI: 10.1186/s11671-021-03517-y.

[49] Alkaykh, S., Mbarek, A., Ali-Shattle, E.E. (2020). Photocatalytic degradation of methylene blue dye in aqueous solution by $MnTiO_3$ nanoparticles under sunlight irradiation. *Heliyon*, 6(4), e03663. DOI: 10.1016/j.heliyon.2020.e03663.

[50] Zhang, L., Jamal, R., Zhao, Q., Wang, M., Abdiryim, T. (2015). Preparation of PEDOT/GO, PEDOT/MnO_2, and PEDOT/GO/MnO_2 nanocomposites and their application in catalytic degradation of methylene blue. *Nanoscale Research Letters*, 10(1), 1–9. DOI: 10.1186/s11671-015-0859-6.

[51] Abdiryim, T., Ali, A., Jamal, R., Osman, Y., Zhang, Y. (2014). A facile solid-state heating method for preparation nanocomposite and photocatalytic activity. *Nanoscale Research Letters*, 89, 1–8. DOI: 10.1186/1556-276X-9-89.

[52] Senatova, S.I., Senatov, F.S., Kuznetsov, D. V., Stepashkin, A.A., Issi, J.P. (2017). Effect of UV-radiation on structure and properties of PP nanocomposites. *Journal of Alloys and Compounds*, 707, 304–309. DOI: 10.1016/j.jallcom.2016.11.170.

[53] Anpilov, A.M., Barkhudarov, E.M., Kozlov, Y.N., Kossyi, I.A., Misakyan, M.A., Moryakov, I. V., Taktakishvili, M.I., Tarasova, N.M., Temchin, S.M. (2019). UV Radiation of High-Voltage Multi-Electrode Surface Discharge in Gaseous Medium. *Plasma Physics Reports*, 45(3), 246–251. DOI: 10.1134/S1063780X19020016.

[54] Sari, M.I., Agustina, T.E., Melwita, E., Aprianti, T. (2017). Color and COD degradation in photocatalytic process of procion red by using TiO_2 catalyst under solar irradiation. *AIP Conference Proceedings*, 1903, 040017. DOI: 10.1063/1.5011536.

[55] Richards, B.S., Hudry, D., Busko, D., Turshatov, A., Howard, I.A. (2021). Photon Upconversion for Photovoltaics and Photocatalysis: A Critical Review. *Chemical Reviews*, 121(15), 9165–9195. DOI: 10.1021/acs.chemrev.1c00034.

[56] Mebed, A.M., Abd-Elnaiem, A.M., Alshammari, A.H., Taha, T.A., Rashad, M., Hamad, D. (2022). Controlling the Structural Properties and Optical Bandgap of PbO–Al_2O_3 Nanocomposites for Enhanced Photodegradation of Methylene Blue. *Catalysts*, 12(2), 142. DOI: 10.3390/catal12020142.

[57] Tzompantzi, F., Mantilla, A., Bañuelos, F., Fernández, J.L., Gómez, R. (2011). Improved photocatalytic degradation of phenolic compounds with ZnAl mixed oxides obtained from LDH materials. *Topics in Catalysis*, 54(1–4), 257–263. DOI: 10.1007/s11244-011-9656-3.

[58] Chakrabarti, S., Dutta, B.K. (2004). Photocatalytic degradation of model textile dyes in wastewater using ZnO as semiconductor catalyst. *Journal of Hazardous Materials*, 112(3), 269–278. DOI: 10.1016/j.jhazmat.2004.05.013.

[59] Sapawe, N., Jalil, A.A., Triwahyono, S., Sah, R.N.R.A., Jusoh, N.W.C., Hairom, N.H.H., Efendi, J. (2013). Electrochemical strategy for grown ZnO nanoparticles deposited onto HY zeolite with enhanced photodecolorization of methylene blue: Effect of the formation of SiOZn bonds. *Applied Catalysis A: General*, 456, 144–158. DOI: 10.1016/j.apcata.2013.02.025.

[60] Kansal, S.K., Singh, M., Sud, D. (2007). Studies on photodegradation of two commercial dyes in aqueous phase using different photocatalysts. *Journal of Hazardous Materials*, 141(3), 581–590. DOI: 10.1016/j.jhazmat.2006.07.035.

[61] Tayyebi, A., Soltani, T., Lee, B.K. (2019). Effect of pH on photocatalytic and photoelectrochemical (PEC) properties of monoclinic bismuth vanadate. *Journal of Colloid and Interface Science*, 534, 37–46. DOI: 10.1016/j.jcis.2018.08.095.